Do It Yourself –

Scanning Tunneling Microscope

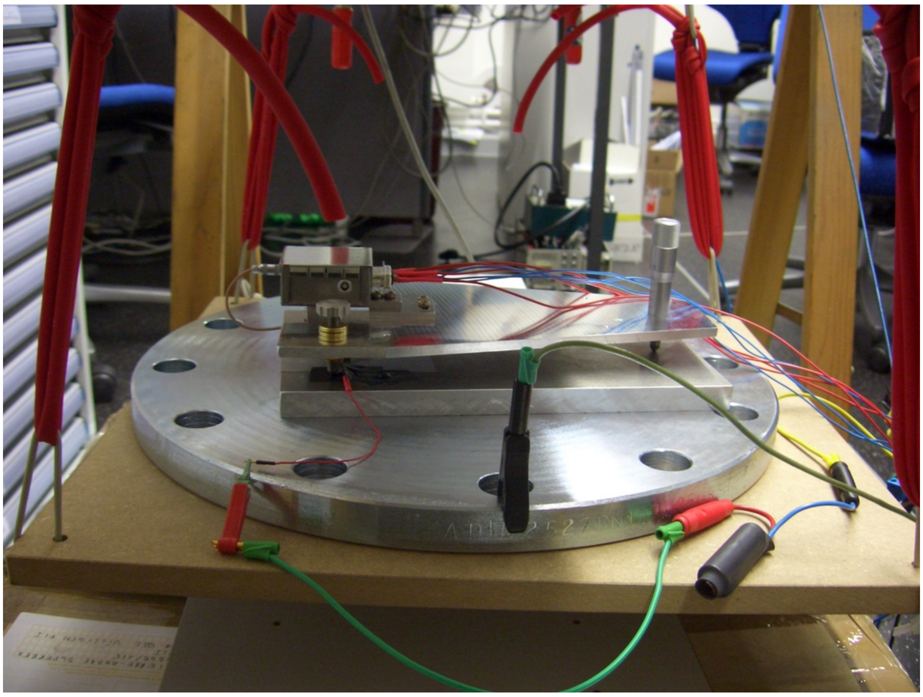

Kantonsschule Wettingen
Maturaarbeit 2008/2009

Authors

Sandro Merkli
Ivan Ovinnikov
Dominik Wild

Advisers

Wolfgang Mann
Dr. Thomas Graf

Preface

Already half a year before the beginning of the *Maturaarbeit*, we had decided what we wanted to do: to build our own scanning tunneling microscope. The idea emerged when we heard that the physical assistant at our school, Hansulrich Schmutz, had bought components to construct such a device. We thought it to be an ideal project for several reasons. The practical work would set a contrast to school and it would be an opportunity to experience research and its creative processes. Furthermore, we are all intrigued by sciences and technology.

We were aware of the fact that our enterprise did not promise definite success. Due to this circumstance, we set our minimal goal to be the following: measure and derive a function of the tunneling current depending on the distance between the tip and the sample. We are glad to have reached this goal but we did not succeed to accomplish our ultimate goal of a fully functioning microscope. However, we plan to continue our project and this work lays a solid base for that. Thus, that we are looking forward to make quick progress. We are also participating in the Schweizer Jugend Forscht competition which sets a different time frame. The deadline set for the competition is a few months later than the Maturaarbeit's deadline. This makes it possible for us to try and achieve our final goals until then.

This paper should give an impression of our work and introduce the reader to the topic of scanning tunneling microscopy. The first part covers the theoretical background whereas the second part specifically documents our implementation of a scanning tunneling microscope. Both parts have their own introduction which will guide the reader. In the third part, we document and interpret the results we have achieved so far. In addition to this paper, we acquired an internet domain (`www.stm-diy.ch`).Under this address, we published a summary of the work we've done and contact addresses for questions. For more detailed information, we provide a downloads section containing useful schematics.

We are greatly indebted to many people and organizations who supported us in our work. The Paul Scherrer Institute, IBM Zurich, EMPA and Carl Zeiss AG all contributed to our project with their generous financial aid. IBM Zurich and the Paul Scherrer Institut both offered their help in technical concerns. The co-operation with the Paul Scherrer Institut turned out to be extremely helpful and we owe special thanks to Jan Hovind, Siegfried Ebers, Dr. Thomas Jung and Valeri Ovinnikov, Ivan's father. He spent a lot of time designing the control electronics, a task not fulfillable for us. Finally, we have to express our gratitude to Hansulrich Schmutz. His experience, explanations and effort were of inestimable value and confirmed us in our enthusiasm. Martin Merkli, Sandros father, helped a lot in the acquisition of non-standard materials used for the mechanical setup, and provided a car, making us a lot more mobile and time-efficient.

Contents

List of Figures

Part I
Theoretical Treatment

This part covers the most important theoretical aspects of scanning tunneling microscopy. Due to the variety of components in a scanning tunneling microscope, the sections in this part are not continuous. For the same reason, the treatment of the single aspects remains rather qualitative. Nevertheless, it should give the reader an insight to challenges and their technical solutions even in topics he is not familiar with.

The introduction gives a short overview about scanning tunneling microscopy and explains the fundamental working of a STM. Section 2, Quantum Tunneling, explores more precisely the physical principles underlying scanning tunneling microscopy. The following four sections concentrate on technical aspects. Section 3, Piezoelectric elements, provides information about how the small movements of the tip can be realized, while section 4 is about the different kinds of electronics which are required for read-out and control. The last two sections, Vibration Isolation and Tip Preparation, shortly comment on two further challenges.

The issues addressed are by no means exhaustive but we do not want to go into more details. Our bibliography refers to relevant literature about scanning tunneling microscopy for further reading. Even these books refer to literature about specific topics as they cannot treat it sufficiently.

1 Introduction

The STM is a powerful device to investigate surfaces and was invented in 1981 by Gerd Binnig and Heinrich Rohrer at the IBM research center in Rüschlikon. Binnig and Rohrer were awarded the Nobel Prize in Physics for this invention in 1986. Figure 1 illustrates the functioning of the STM. A very sharp probe – in the best case, there is a single atom at the end – scans the surface from a very small distance, usually in the order of an atomic diameter. The scanning motion is controlled with piezoelectric elements (3 Piezoelectric elements, page 10). Due to a quantum physical phenomenon called tunneling effect, the voltage between probe and sample leads to a very small current (2 Quantum Tunneling, page 6). Information about the surface can be obtained by measuring this current as it depends on electrical properties of the sample and on the distance between the tip of the probe and the sample.

In general, there are two ways to scan a surface. Either the vertical position of the probe or the current is kept constant. The former only works on very flat surfaces but allows a high scanning speed. It is mainly used to study dynamic processes. The latter requires a feedback circuit to adjust the vertical position of the tip such that there is no risk that the tip could crash into the sample. At the end, an image is generated from the x-y-z-coordinates of the tip (constant current) or the x-y-coordinates and the current (constant distance). Good STMs can even resolve single atoms. Figure 2 shows an image of a graphite surface with atomic resolution.

There are other applications of the STM such as tunneling spectroscopy which is out of the scope of this project. STMs only work on conducting surfaces. The are other microscopes of the same type, the family of scanning probe microscopes, which can scan non-conducting surfaces. The most important one in this family is the atomic force microscope. The principle of scanning is the same but it measures force, rather than current.

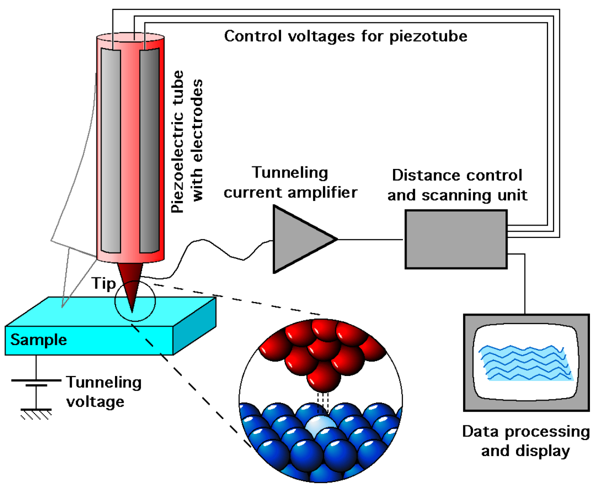

Figure 1: Schematic diagram of a STM. `http://en.wikipedia.org/wiki/Image:ScanningTunnelingMicroscope_schematic.png` (January 8, 2009)

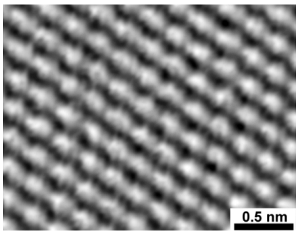

Figure 2: STM scan of a graphite surface with atomic resolution.
http://de.wikipedia.org/w/index.php?title=Bild:Graphite_ambient_STM.jpg
(January 8, 2009)

2 Quantum Tunneling

In order to understand the tunneling effect, we first consider the classical behavior of particles. As a simplification we use a one-dimensional model. The motion of a particle with energy E in a potential $E_{pot}(z)$ is described by

$$E_{kin} = \frac{1}{2}mv^2 = E - E_{pot}(z)\,,$$

where m is the mass and v the velocity of the particle. v has a real result for $E - E_{pot}(z) \geq 0$. Therefore an area with potential $E_{pot} > E$ is impenetrable by classical laws.

At the beginning of the 20$^{\text{th}}$ century, quantum mechanics revolutionized the physical understanding of matter. On the one hand it was found out that light did not only show wave-like behavior. Rather it had to be described as a stream of particles, the photons, to explain some experiments. On the other hand exactly the opposite was stated for particles. *All matter has a wave-like nature.* This statement is called *De Broglie hypothesis* in honor to Louis de Broglie who stated it in his PhD thesis in 1924 and received the Nobel Prize in Physics in 1927 for his work. The wavelength of matter waves is described by the equation

$$\lambda = \frac{h}{p}\,.$$

h is Planck's constant having the value $6.626069 \cdot 10^{-34}$ J s and p is the particle's momentum. The equation tells us why the wave-like behavior of matter cannot be observed in everyday life. Let us take the example of a tennis ball weighing 57g and flying at a speed of 40 $\frac{\text{m}}{\text{s}}$. We get a result of $\lambda = 2.906 \cdot 10^{-34}$ m which is far too small that any effect caused by the wave-like nature would be observable. However on small scales or very low temperatures it is measurable and definitely not negligible. Many phenomena on atomic scale, such as the tunneling effect, can only be explained with the help of quantum mechanics.

A particle in quantum mechanics is described by the wavefunction $\psi(z)$ satisfying the Schrödinger equation. The Schrödinger equation was postulated in 1926 by the Austrian physicist Erwin Schrödinger. It is a differential equation, which means it states a relationship between a function and its derivative. Actually, the Schrödinger equation is a second order differential equation, containing the second derivative.

$$\frac{d^2\psi(z)}{dz^2} = -\frac{2m}{\hbar^2}(E - E_{pot})\,\psi(z)$$

is the so-called time-independent version of the Schrödinger equation. $\hbar = \frac{h}{2\pi} = 1.054 \cdot 10^{-34}$ Js is a constant often used to simplify equations. The time dependent version, often denoted as Ψ, is more complex (also in the mathematical sense of the word) but it is not required in order to understand the tunneling effect. There is a relation between the wavefunction and the probability for the particle to stay in a certain region of space. The continuous probability distribution $P(z)$ equals the wavefunction squared.

$$P(z) = (\psi(z))^2$$

Applying the Schrödinger equation, it is possible to calculate the wavefunction of an electron in a model similar to the situation in a STM. We take the potential of the probe as point of reference. The electrons have a positive energy of E since they are moving in the solid. ϕ is the work function of the material. It is defined as the minimum energy required to remove an electron from the material [1]. E is smaller than ϕ because otherwise the electrons would not be bound to the metal. Figure 3 shows a graph of this situation.

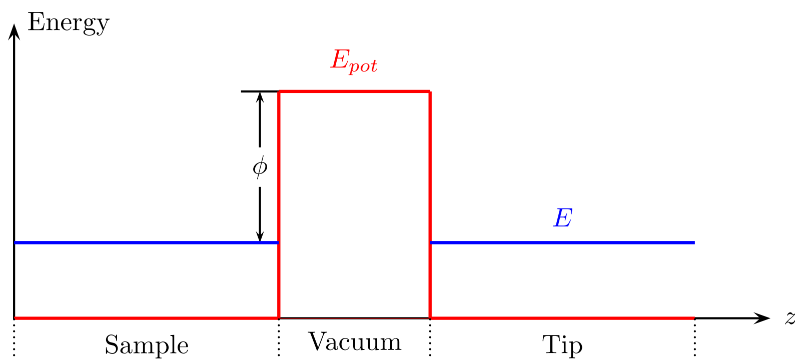

Figure 3: Potential energy in a STM. Own illustration.

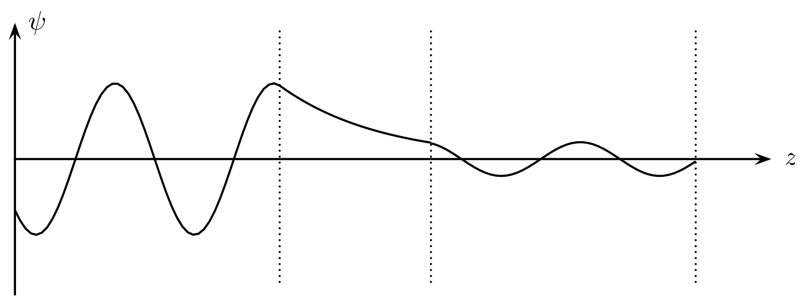

Figure 4: Wavefunction of an electron in the sample. Own illustration.

The Schrödinger equation has two principally different solutions. Figure 4 shows how these solutions apply in the model of the STM.

$$\boxed{\begin{aligned}\psi(z) &= A\cos(kz+\delta) && \text{if } E-E_{pot}>0\\ k^2 &= \frac{2m}{\hbar^2}(E-E_{pot}) &&\\ \psi(z) &= Be^{-\kappa z} && \text{if } E-E_{pot}<0\\ \kappa^2 &= \frac{2m}{\hbar^2}(E_{pot}-E) &&\end{aligned}}$$

We do not show how to derive these results. Nevertheless, one can easily verify them by putting ψ back into the Schrödinger equation. We denote the wavefunction in the sample, the vacuum and the tip as $\psi_1(z)$, $\psi_2(z)$ and $\psi_3(z)$, respectively. ψ depends on the amplitude A and the phase shift α. Analogously, ψ_3 depends on C and β. As a fifth parameter, there is B in ψ_2. These five parameters can be reduced to one, here A, considering the constraint that the complete wavefunction of the electron has to be continuous. The first two conditions are received by equating the functions at the points where they meet, the other two by equating the derivatives. The gap between sample and tip begins at $z=0$ and ends at $z=d$.

$$\begin{aligned}\psi_1(z) &= A\cos(kz+\alpha)\\ \psi_2(z) &= Be^{-\kappa z}\\ \psi_3(z) &= C\cos(kz+\beta)\end{aligned}$$

$$\begin{aligned}A\cos(\alpha) &= B && \text{(I)}\\ -kA\sin(\alpha) &= -\kappa B && \text{(II)}\\ Be^{-\kappa d} &= C\cos(kd+\beta) && \text{(III)}\\ -\kappa Be^{-\kappa d} &= -kC\sin(kd+\beta) && \text{(IV)}\end{aligned}$$

$$\begin{aligned}\tan(\alpha) &= \frac{\kappa}{k} && \text{(II) : (I)}\\ \tan(kd+\beta) &= \frac{\kappa}{k} && \text{(IV) : (III)}\end{aligned}$$

$$\begin{aligned}\alpha &= kd+\beta = \arctan\frac{\kappa}{k}\\ \beta &= \arctan\frac{\kappa}{k} - kd\\ B &= A\cos(\alpha) = A\cos\left(\arctan\frac{\kappa}{k}\right) = A\frac{k}{\sqrt{k^2+\kappa^2}}\\ C &= \frac{B}{\cos(kd+\beta)}e^{-\kappa d} = \frac{B}{\cos(\alpha)}e^{-\kappa d} = Ae^{-\kappa d}\end{aligned}$$

$$\boxed{\begin{aligned}\psi_1(z) &= A\cos\left(kz + \arctan\frac{\kappa}{k}\right)\\ \psi_2(z) &= A\frac{k}{\sqrt{k^2+\kappa^2}}e^{-\kappa z}\\ \psi_3(z) &= Ae^{-\kappa d}\cos\left(kz + \arctan\frac{\kappa}{k} - kd\right)\end{aligned}}$$

Astonishingly the wavefunctions are not zero, neither in the tip nor in the vacuum. This means that it is possible that an electron from the sample overcomes the barrier and *tunnels* to the probe. Figure 5 shows the probability function of the electron. Although small, there is a probability that the electron stays in the tip. It can be seen from the result for $\psi_3(z)$ that the tunneling probability is proportional to $e^{-2\kappa d}$, the amplitude of the probability function in the tip. By classical laws the crossing of the barrier is not possible. Tunneling cannot be explained by classical physics but only by quantum mechanics.

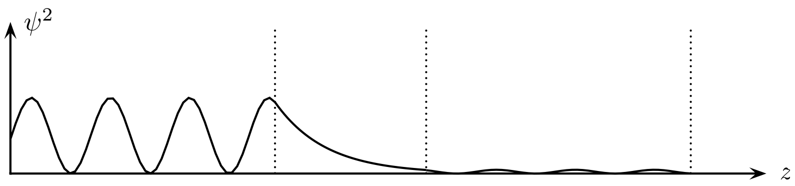

Figure 5: The probability function of the electron in Figure 4. Own illustration.

Still there is no measurable current without a voltage applied because electrons tunnel equally from the tip to the sample and vice versa. With a voltage one side is put onto a higher potential. The electrons on this side have a greater probability to tunnel than the ones in the lower potential. This results in a net current which is measured in a STM. The current is proportional to the probability of tunneling.

$$\boxed{I \propto e^{-2\kappa d}}$$

A typical value for $E_{pot,vac} - E = \phi$ (the work function) is 5 eV [11]. Together with the electron mass $m = 9.109 \cdot 10^{-31}$ kg, we can use this value to calculate a numerical estimate for the decrease of the tunneling current with distance.

$$\kappa = \frac{\sqrt{2m\phi}}{\hbar} = 1.146 \cdot 10^{10}\,\frac{1}{\text{m}}$$

For a distance d of 1Å (10^{-10} m), this gives for the current

$$I \propto e^{-2\kappa d} = e^{-2.291} = \frac{1}{9.886}\,.$$

Thus, the current decreases by roughly one order of magnitude per 1Å. This value is only true in the vacuum. In air, the workfunction is much smaller because water condensates on the probe and tip (see section 12 for more information).

3 Piezoelectric elements

3.1 The piezoelectric effect

The piezoelectric effect is a property of certain crystals and ceramics. If piezoelectric materials are compressed, an electric field in direction of the acting force occurs. This effect is called the direct piezoelectric effect. The converse piezoelectric effect is the elongation of a material if a voltage is applied. Pierre and Jacques Curie were the first to demonstrate the piezoelectric effect in 1880 [7]. Quartz is an example of a piezoelectric material and it is widely used in watches and clocks as oscillator. Another well-known application are piezoelectric crystals as igniter of lighters. A hammer hits the crystal thereby producing a voltage of thousands of volts which creates a spark [7].

In a STM, stacks of piezoceramics are used to control the position of the probe. Such piezostacks consist of layers of a piezoceramic material with electrodes separating the layers. The single layers are therefore serially coupled and the effect is amplified. There are two important constants describing the properties of piezoelectric materials. Figure 6 shows a piezoelectric element in a homogeneous electric field E_3 parallel to the z-axis. The element not only expands along the z-axis but also contracts in x-direction. The relative changes in length are

$$S_1 = S_x = \frac{\Delta x}{x}$$
$$S_3 = S_z = \frac{\Delta z}{z}.$$

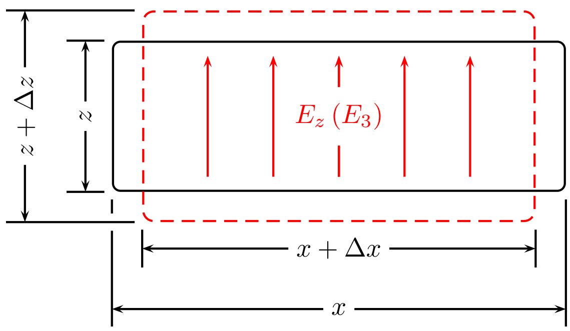

Figure 6: Illustration of the piezoelectric coefficients. Own illustration (inspired by [1]).

In the standard convention x, y, z are labeled with 1, 2 and 3. The so-called piezoelectric coefficients are the relative expansion divided by the electric field. The first number of the index is the direction of the field, the second one the direction of the expansion.

$$d_{31} = \frac{S_1}{E_3}$$
$$d_{33} = \frac{S_3}{E_3}$$

Using the relation $E_3 = \frac{U}{z}$ we get

$$\Delta x = d_{31}\, U\, \frac{x}{z}$$
$$\Delta z = d_{33}\, U$$

3.2 Scanner Types

Two scanner types used in STMs are worth to be mentioned. The tripod scanner consists of three piezoelectric bars arranged in a tripod. It was implemented in the first STM by Binnig and Rohrer and is still used in some home-built STMs. A tube scanner is a piezoelectric tube with four electrodes on the outer and one on the inner side. It can be bent by applying a voltage to two opposite electrodes. The elongation (z-direction) is controlled using the fifth electrode inside the tube. The tube has several advantages over the tripod scanner and is therefore more often used in professional microscopes. The resonance frequency of tube scanners is higher than the one of tripod scanners and, in addition, it is simpler in operation.

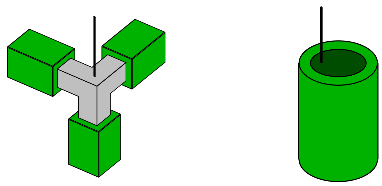

Figure 7: The tripod and the tube scanner. Own illustration.

4 Electronics

4.1 Amplification

The small tunneling current, in the order of pico- to nanoamps, needs to be amplified to be measurable. The current should also be converted into into a voltage since voltages are less sensitive to noise and can be easier processed. An amplifier that transforms a current into a voltage is called transimpedance amplifier. A technical solution is offered by operational amplifiers (op-amps).

4.1.1 Operational Amplifiers

Op-amps are electronic components available in all different colors and shapes (Figure 8). Standard op-amps are a mass product and therefore very cheap. Op-amps with the specifications required for the application in a STM are more expensive but there is still a number of products to choose from, different manufacturers included. Due to the versatility of op-amps, they are used in a vast array of devices.

Figure 9 shows the circuit board symbol of an op-amp with its most important pins. U_{s+} and U_{s-} are the power supply pins. The voltage at the pins is very often $\pm 15\,\mathrm{V}$, which also defines the maximum output voltage. U_+ and U_-

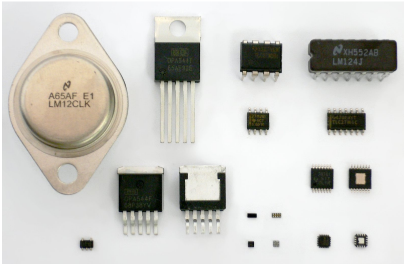

Figure 8: A number of different op-amps. http://upload.wikimedia.org/wikipedia/commons/0/06/OPAMP_Packages.jpg (January 8, 2009)

are the non-inverting and the inverting inputs respectively. U_{out} is the output pin. In an ideal op-amp the input resistance, the resistance between U_+ and U_-, is infinite, so is the gain factor G. The output resistance is zero. These values are practically impossible but the properties of real op-amps are actually close to the ideal ones.

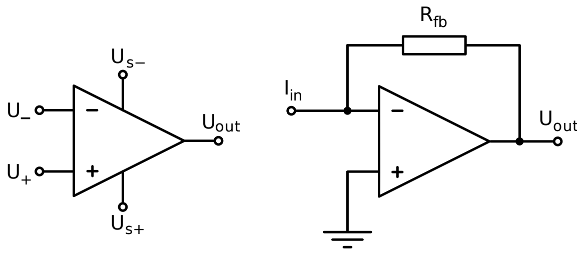

Figure 9: The circuit board symbol of an op-amp (left) and an op-amp as a current amplifier (right). Modified from http://upload.wikimedia.org/wikipedia/commons/9/97/Op-amp_symbol.svg (23.11.2008)

An op-amp as shown on the left hand side of Figure 9 amplifies the input voltage $U_+ - U_-$ by the gain factor G.

$$U_{out} = (U_+ - U_-)\, G$$

This is useless since G is very high and weak noise is already amplified to the maximum output voltage. However, there are many different op-amp circuits such as the logarithmic or the differential amplifier which render the op-amp so flexible. Most relevant for the application in a STM is the transimpedance amplifier or current amplifier also shown in Figure 9. The working of this circuit can be derived from Kirchhoff's laws but at this place, a good approximation shall be enough. From [1]:

> To a very good approximation, the output voltage should provide a feedback current through the feedback resistance R_{fb} to compensate the input current such that the net current entering the inverting input of the op-amp is zero. The non-inverting input is grounded, and the voltage at the inverting input should be equal to ground. This implies
>
> $$U_{OUT} = -I_{IN} R_{FB}$$

A common value for R_{fb} in order to achieve sufficient amplification is $100\,\mathrm{M}\Omega$. This gives a gain factor of $0.1\,\frac{\mathrm{V}}{\mathrm{nA}}$. A gain of $1\,\frac{\mathrm{V}}{\mathrm{nA}}$ is often desirable [1]. Since feedback resistances greater than $100\,\mathrm{M}\Omega$ may cause technical problems, the amplification is often implemented as a cascade of two amplifiers.

There are other issues regarding amplification such as noise and frequency response. All of these topics are thoroughly covered in [1]. It is important to know that noise and other technical aspects, for instance parasitic capacities, are limiting factors of the amplifier.

4.2 Control Electronics

The amplified signal from the tunneling amplifier has to be read out and the position of the z-piezo must be adapted accordingly if running the STM in constant current mode. Principally, there exist two different implementations of such a feedback loop, an analog and a digital one. Figure 10 shows a schematic drawing of two such implementations.

The analog feedback circuit consists of a logarithmic amplifier and some feedback electronics which compare the output signal to a set-point value and return a signal to the high voltage amplifier driving the piezos. In the feedback electronics a differential amplifier amplifies the difference between the output voltage and a set-point value. This value is then integrated since the difference between the set-point current and the measured current refers to a deviation from the current position of the tip. Therefore the value of the differential amplifier has to be added to the voltage at the z-piezo. This is exactly what is done by an integrator. The logarithmic amplifier, the differential amplifier and the integrator can all be realized as op-amp circuits, which makes the analog feedback quite simple.

For a fully functional STM, the x- and y-piezos must be controlled as well and the signal must be read out. Both can be accomplished by different means. In the first STMs, the scanning signal was produced using function generators, nowadays computers in combination with a digital to analog converter (D/A converter) can take this task. The output signal is often read out using an analog to digital converter (A/D converter) but it could also be analyzed with simpler means such as an oscilloscope.

In a digitally controlled feedback, all the steps after the current amplifier are replaced by an A/D converter, D/A converter and a computer, usually a microcontroller. The signals from the current amplifier are converted to digital signals and registered by the microcontroller. They can be later transmitted to a personal computer. The microcontroller compares the value to a set-point value and returns a corresponding voltage to the high voltage amplifier via a D/A converter.

The great advantage of digital implementation is its versatility. Other parameters such as the x- and y-piezos and the bias voltage can be controlled using the same platform. Modifications of the scanning procedure can be controlled by software. However, it is more complicated than an analog implementations and especially the speed of the platform can pose a problem. The real-time requirements ask for special solutions, i.e. a microcontroller, and are hard to fulfill with a PC.

An effect to be considered in both approaches is the delay in response of the system. There is a delay in every amplifier, in the converters and in the microcontroller. Neither do the piezos respond instantaneously due to mechanical inertia. Therefore, the gain of the feedback circuit cannot be chosen arbitrarily high. If the gain is chosen too high, the tip moves to its new position while the position is corrected even more so that at the end the tip is too far away or too close. The whole process starts into the other direction. The response is underdamped and the tip oscillates. It is easiest to find the critical damping by experiment.

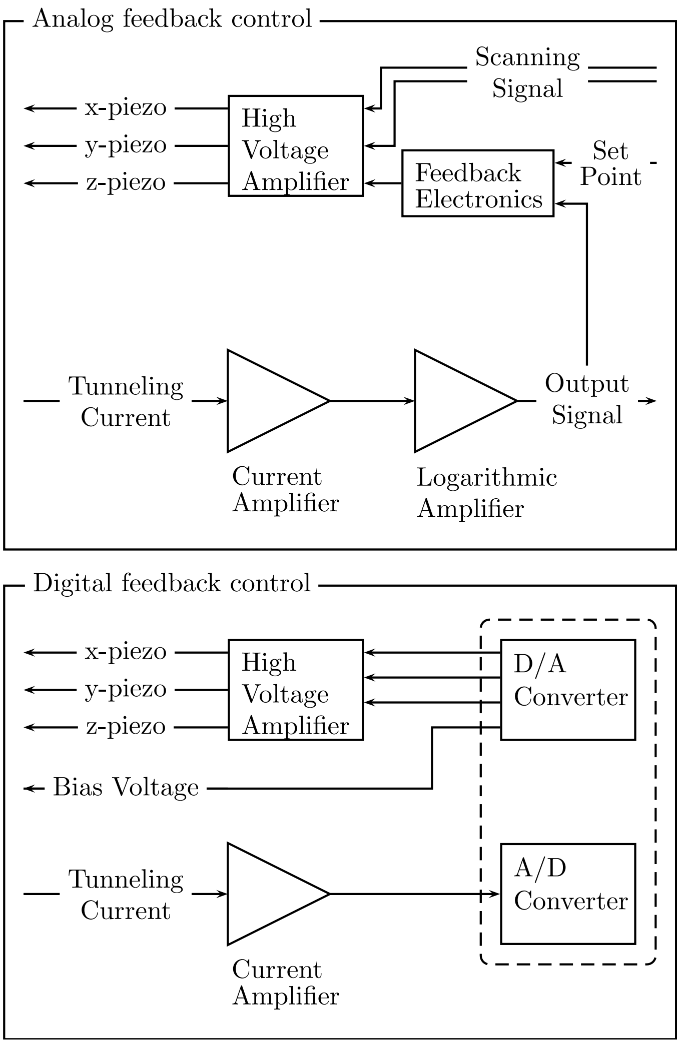

Figure 10: Typical implementations of analog and digital feedback control. Own illustration (inspired by [1]).

5 Vibration Isolation

In order to achieve high resolution, the STM should be insensitive to external vibrations. The sources of vibrations can be various, from acoustic noise to a street running nearby. Therefore, the required damping also depends on the environmental circumstances. Without any calculation, one can understand that a rigid design is the most important factor in vibration isolation. The vibrations do not influence the measurement if all parts of a STM vibrate at the same frequency and amplitude. Springs together with a viscous damper, the damping force is proportional to the speed of the spring, can be completely sufficient. Sometimes, in a very quiet environment, no damping at all is required. Two stage systems can provide even better damping but the overall gain in performance is limited so the focus should be on a rigid design. There are many different approaches to vibration isolation, some of them dedicated to special working conditions such as ultra high vacuum. Exploring their advantages and disadvantages would incorporate long calculations with doubtable success since many insights are based on experimental experience.

6 Tip Preparation

Ideally, there should be a single atom at the end of the tip to achieve maximum resolution. This proves to be less critical in experiment than expected. Since the tunneling current shows an exponential behavior, a single atom being a bit closer to the surface than others is responsible for most of the current flowing. Most tips are made of a Platinum-Iridium alloy or of tungsten. Platinum-Iridium does not easily oxidate and is therefore often used under ambient air conditions. The tips can be prepared using a side cutter, half drawing, half cutting under an acute angle. Tungsten tips are sometimes etched which gives a better control over the resulting tip. Another suitable way to get a good tip is to apply a relatively high voltage between tip and sample while scanning which draws a single atom out of the surface which is than attached to the tip.

Even with a seemingly good tip, atomic resolution is not always given. It can occur spontaneously during a scan, even after a crash with the surface.

Part II
Documentation

The documentation of our work illustrates our implementation and process to achieve it. In this documentation we follow a structure which aims to emphasize the process of improvement and problem solving. In the section Initial Approach, we explain our initial plans how to build the STM. This part is held relatively short concerning the mechanics whereas the complexity of the electronics require a longer introduction. As expected, various difficulties arose in the course of our work. The attempt to minimize their negative influences, whether they were successful or not, were reason for changes in the design we used in the beginning. All these difficulties and changes are subject in the second section, Difficulties. The third section, Current Design, summarizes the state after all the improvements made. As we are participating in the competition hosted by *Schweizer Jugend forscht* and due to our personal ambition, the end of the *Maturaarbeit* is not the end of our work. Hence, our future plans are mentioned in section 10, Future plans.

We hope this allows insight to our working process and perhaps even helps other amateur STM-builders in their enterprise.

7 Initial Approach

7.1 Mechanical Build

When building our STM, we initially kept really close to a reference design we had found during our research on the internet [10]. The main reason for this is that a full design of a microscope would simply require too much time to realize. Figure 11a shows the body of our STM. The reference design is based on a construction which contains two aluminium plates, one lying on top of the other with a three-point support. All three heights can be adjusted via fine approach screws. The scanning head is mounted between two of the screws, with an adjustable distance to the line connecting the two. This design makes the lever applied by the third screw at the back user-adjustable, which is convenient. The coarse approach of the tip is done using the screw at the back. For oscillation damping, we intended to use a metal plate with a weight of about 30 kg placed on a pneumatic tire semi-filled with air (Figure 11b). A simple cardboard box with cone foam isolation was supposed to acoustically isolate the microscope.

All mechanical parts, safe for the two parts of the scanning head, were manufactured by us at school. Material and instructions on how to use the machine were provided by the school's assistant of the physics department, Hansulrich Schmutz, who soon became our main consultant in terms of mechanical parts. Due to their diminutive size, production of the scanning head parts had to be outsourced to Jan Hovind from PSI. The heavy metal plate was bought in a store in Wettingen pointed to by Martin Merkli. The actual use of such plates is to close pipes that will be under pressure. As the plate was very dirty, we sent it to galvanizing using a contact of Martin Merkli's. The wooden board was easily obtained at a local do-it-yourself store and cut down to size at purchase.

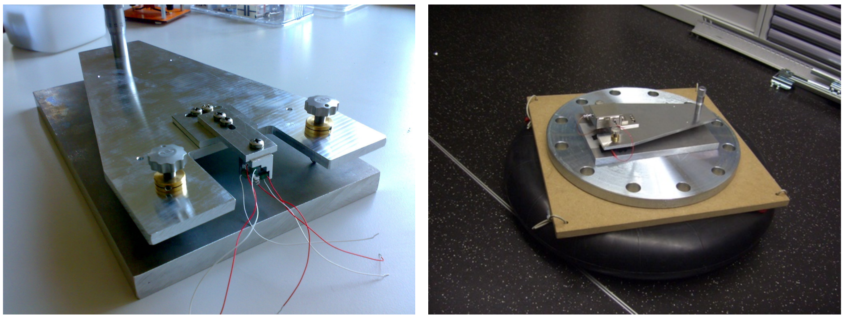

(a) Mechanical build (b) Vibration damping

Figure 11: Two pictures illustrating our approach. Own pictures.

7.2 Tunneling Current Amplifier

At the beginning of our experiments, we used an amplifier which we had received from Siegfried Ebers, an electronics engineer at PSI. The amplifier was designed to amplify signals from photodiodes in order to detect radioactive radiation. Both the amplification of the tunneling current and of photodiodes deal with high resistances at the input and very small currents. The amplifier was built on a printed circuit board and included a two-stage amplification and a DC/DC converter so that it was not depending on a $\pm 15\,\mathrm{V}$ power supply. To shield the amplifier, we fabricated a custom enclosure at the school's mechanical facility. Starting off from a commercially available enclosure for 2.5 inch hard drives, we added custom front and back plates, having drilled holes for inputs and outputs into them.

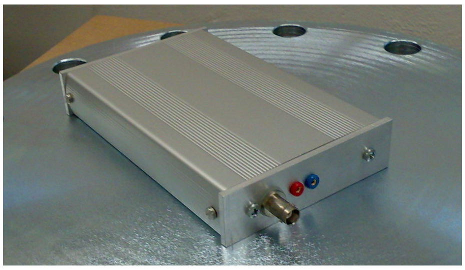

Figure 12: Picture of the body of the first amplifier in its case. Own picture.

7.3 Scanning Electronics

Perhaps the most complex part of our project are the electronics required to scan the surface of the sample. We chose the digital approach as described in section 4, based around a microprocessor and digital-to-analog and analog-to-digital signal converters. Due to our lack of knowledge and experience, the schematics were drawn by Valery Ovinnikov using the P-Cad 2006 Suite. The design of the printed circuit board, however, was largely our work with a revision by a specialist, who, in our case, was again Valery.

7.3.1 Components

The integral part of the control electronics is the microprocessor or microcontroller used for the feedback loop. We chose the PIC32 Microprocessor produced by Microchip due to its versatility and connectivity. The PIC32 USB Starter Kit board consists of the microprocessor itself, a fast USB interface for communication with the host PC, a JTAG debugging port and a 120-pin I/O connector to transfer signals coming from the D/A and A/D converters.

For the D/A converter we used the DAC8814 chip produced by Texas Instruments (TI). It features four independent 16-bit channels, which is suitable for our purposes - 3 channels are dedicated for each of the piezo actuators and another one for the regulated bias voltage. The 16-bit A/D converter chip used for the conversion of the output from the current amplifier (ADS8321) is also manufactured by TI. The reason for choosing the 16-bit resolution is that it theoretically permits very detailed scans. Due to external factors however, it is impossible to achieve such a resolution with the current mechanics while maintaining the precision of the scan.

Another important section of the circuit design are the power amplifiers - OPA551 by TI - which provide the high voltages required by the piezo drivers, thus enabling their control from the host PC.

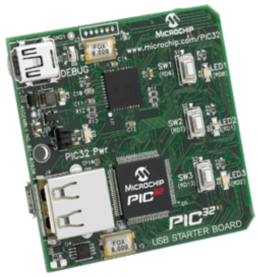

Figure 13: PIC32 Microprocessor Board. http://www.microchip.com/stellent/images/mchpsiteimages/USBStarterBoard_oblq.png (January 8, 2009)

To supply the components with power, we acquired a linear power supply. The benefits of a linear power supply over a switched one is the relatively low noise output, which plays a crucial role in our case, since we work with extremely small signals. The linear power supply helps keeping the noise at a minimum. Due to the fact that the components require an array of different voltages, we initially thought of procuring a power supply with a regulated multiple voltage output. Unfortunately, such a device turned out to be quite expensive and rare. Therefore, we settled with an unregulated linear power supply providing ±32V, which are then transformed into the required values by passing the initial voltages through a series of voltage converters.

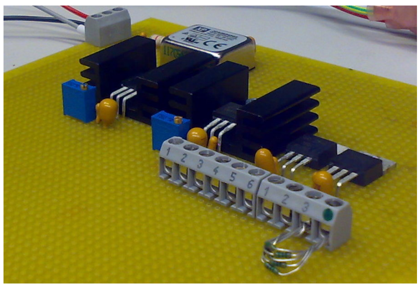

Figure 14: Voltage converters. Own picture.

7.3.2 PCB Design

Instead of using a prototype board, which would be a simpler approach, we decided to design a proper printed circuit board to host our components. The software used is part of the P-Cad 2006 Suite, provided by the Paul Scherrer Institute.

Our PCB consists of four layers: two signal layers (Top and Bottom), AGND, the analog ground layer and '−15V' – a power layer. It needs to be noted that both the AGND and the −15V layers include alterations – the AGND layer is split up into analog and digital ground and contains a +15V and a +5V power line. The power layer consists of the −15V and ±24V power planes.

The design of printed circuit boards generally consists of two tasks - the placing of the components onto the board and the routing of the connections between the single components. To begin placing components, a netlist must be generated. The netlist contains the information on the components it draws from the schematic. This information consists of the component's name, connections and the PCB pattern - its real-life dimensions and pin designators. When generating a netlist, an automatic error check takes place, ensuring the conformity of the design to electric rules, such as checking for possible short circuits.

When placing components, it is best to avoid the entanglement of unrouted connections - this contributes to the overall simplicity of the design and helps to prevent unnecessary routing problems. To route the connections, a variety of autorouters may be used, in our case we chose SPECCTRA, one of the more sophisticated autorouters available. It is also possible to route the connections by hand, however this requires a lot of time and skill. Nowadays, manual routing is mostly used for small alterations and improvements to the automatic routing. While working with our board, it was necessary for adjustment of vias and *loose* connections - connections which the autorouter failed to route.

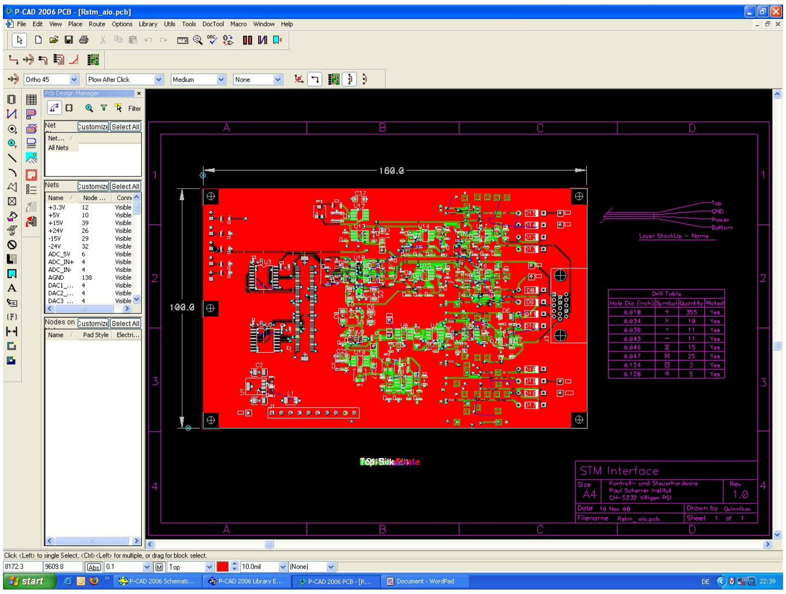

Figure 15: P-CAD 2006 PCB Designer. Own picture.

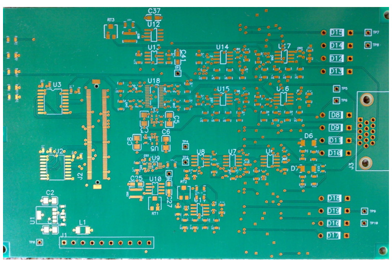

Figure 16: Empty Printed Circuit Board. Own picture.

8 Difficulties

8.1 Vibration Damping

Section 5 concludes that the need for vibration damping depends on how rigid the design of the STM is. The big size of our STM is a disadvantage concerning rigidity, so we required an effective damping. Our first approach consisted of the aforementioned air-filled tire and heavy metal plate but further experimentation deemed this solution to be too sensitive to vibration. We therefore decided to take a different approach using elastic strings (Figure 17). This build seemed more efficient than the other, though further improvements had to be done. When hanging the heavy metal plate from elastic strings, the proportions of the stand proved to be a determining factor. Using a ladder (Figure 17a), the feet are too close to each other, allowing for the whole build to swing sideways. With wooden stands (Figure 17b), the feet are further apart, stabilizing the microscope a lot more. The influence of outside oscillation was sufficiently reduced such that the tunneling current would not be strongly influenced. The elastic strings used are actually designed for body fitness training and elongate a lot, but using multiple strings for every corner eliminated this problem altogether. As a backup for when one of the strings would tear apart, a solid cardboard box just centimeters beneath the hanging plate was used. The length of the strings seemed unimportant but both external advice and our experimentation showed that they needed to be loaded to their limit. This makes the strings harder and less prone to change their length when more or less force is applied.

(a) Hanging from a ladder. (b) Hanging from wooden stands.

Figure 17: The ladder was only a provisional, less effective stand which we later replaced by more stable ones. Own pictures.

8.2 Acoustic Noise

Acoustic noise negatively influenced the stability of the tunneling current which is also related to the big size of the STM. Following an expert's advice, we built a box lined with cone foam. However, when applied, the tunneling current was still very sensitive to acoustic noise. Our only temporary solution to it was to get the environment of the microscope to be as quiet as possible. The design of a new box using glass wool and aluminium foil improved noise cancellation a lot, so much in fact that quiet speaking around the microscope during experimentation did not negatively influence a measurement. The noise cancellation box introduced another difficulty in handling though, as putting it over the microscope after successful approaching of the tip to the sample often ruined the approach. It either crushed the tip into the sample or distanced the tip so far that there was no tunneling current measurable anymore. Yet very careful handling of the box and microscope allowed for some successful experiments, which in turn were a lot more stable.

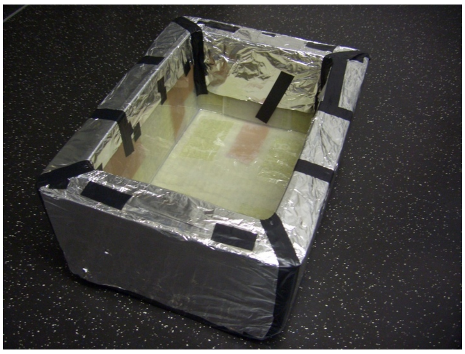

Figure 18: Sound isolation box. Own picture.

8.3 Tunneling Current Amplifier

In experiment, the amplifier turned out to be too slow and noise was on a critical level even though we had put the amplifier into a metal case to shield it. We conducted tests with a $10\,\mathrm{G\Omega}$ resistor and in situ with the microscope. When we removed some capacitors to increase the speed, the noise became unacceptably high. Since we could not locate a problem in the circuit, we decided to build a new amplifier.

We also had to construct a provisional case for the new amplifier, allowing us to test it. It performed well even though it was by far not as elaborate as the first amplifier. After this success, we built a more durable case and a third improved amplifier. The case was manufactured by us from a stock box of that size, adding the connectors and soldering the cabling inside. It features a VGA plug to connect it to the control electronics. Furthermore, there is a plug for the piezos which is internally wired to the VGA connector. The amplifier itself was soldered from the individual parts on a test board and set into the box afterwards. As an improvement from the second amplifier, we added capacitors at the power supply lines to filter noise from the supply. Figure 20 shows the schematic of the amplifier circuit.

The acquisition of the low-noise opamps was surprisingly uncomplicated. The first amplifier used an OPA 111, the second an OPA 129 and the third one an OPA 124, all of them produced by Burr Brown, Texas Instruments. From the data sheets one can easily tell whether an amplifier is suited for an application. Furthermore, there are sample applications on most data sheets. It is good to know that free samples of most opamps can be ordered.

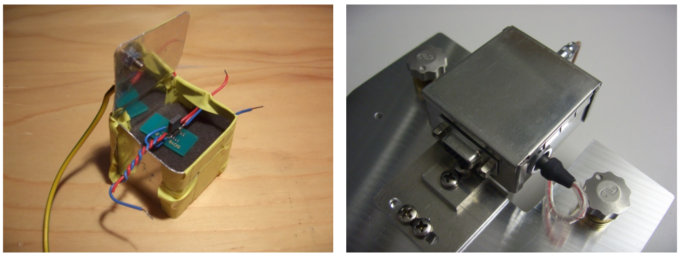

Figure 19: The second and the third amplifier, which could be directly mounted onto the STM. Own pictures.

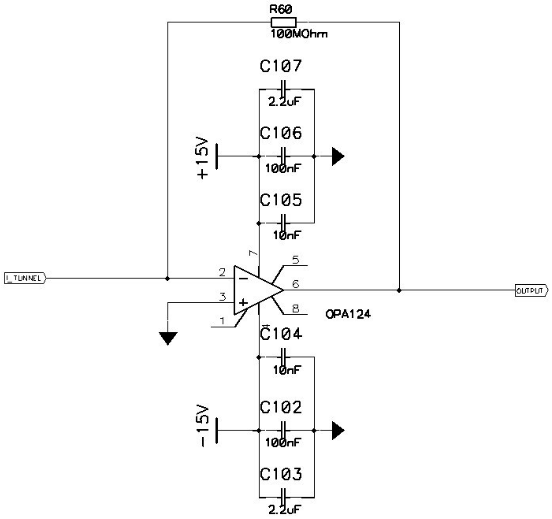

Figure 20: Schematic of the third amplifier. Own picture.

8.4 Control Electronics

We have encountered several problems in the course of designing the board. Since P-Cad has been discontinued, the component libraries are not updated anymore, resulting in a lack of information concerning some of the components. To solve this, we needed to draw some of the components ourselves, as some of the patterns were nowhere to be found. Especially the female part of the 120-pin I/O connector of the PIC32 board proved to be a challenge. Another problem had to do with the routing - due to the somewhat wrong placement of the components, some of the power lines were barely reachable for other components and therefore had to be readjusted. Further difficulty arose when our board was rejected by Eurocircuits because of the insufficient diameter of the vias - connection channels from one layer to the other. This required further customization of the autorouted connections from our side. After resizing the vias and refitting some of the components, the problem was solved.

9 Current Design

After all the manipulations done by us in the course of improving the scanning results, the following design is currently giving us the best results so far.

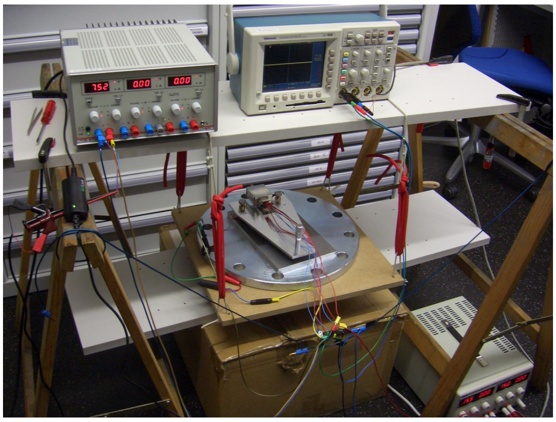

Figure 21: A picture showing the complete design. Own picture.

Damping is now dealt with by elastic ropes and the heavy metal plate, and most of the noise-related problems vanished after the production and usage of the new, improved noise cancellation box. Some trouble still exists, though. The main problem is the vibration caused by us putting the box over the microscope after the coarse approach. This could be solved by using a remotely controlled stepping motor for the coarse approach. This would allow for the box to be put over the microscope before the coarse approach – the coarse approach to be begun only after all vibration has seized.

The latest amplifier works well with relatively little noise. The direct mount onto the STM body and the different connectors simplify the usage. There is only one cable connecting the STM to other devices – now oscilloscopes and power supplies, later the microcontroller interface.

In terms of control electronics, we have successfully produced a uniform control box containing the hand-soldered printed circuit board, the voltage regulators and power supply. Currently, the board is calibrated and the communication between the processor and the DAC and ADC channels is enabled, theoretically allowing us to perform scans.

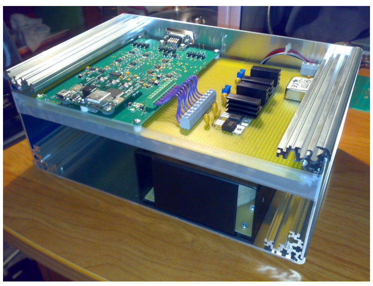

Figure 22: The control electronics in the opened box. Own picture.

10 Future plans

10.1 Mechanical Build

The mechanical build still incorporates certain faults which we are in the course of improving. The inclusion of a stepping motor and linked to this the change of the form factor to a smaller lever is in conception, and a floor board for the noise cancellation box to further enhance its effect is in production.

10.2 Control Electronics

From the present standpoint, we have fully accomplished the task of producing the hardware necessary for the scanning of the sample. To be able to actually generate the scans, the following software must be developed:

- A VISA-compliant USB Class for the communication between LabVIEW and our microprocessor and thus the transfer and processing of raw data coming from our board
- An algorithm managing the scanning signals and reading the data coming from the A/D converter
- A LabVIEW Virtual Instrument which would allow us to process the data and display the scan

Due to the complexity of the USB protocol, it has been proposed that Valery would take over the development of the USB class, allowing us to concentrate on the other two programming tasks.

Part III
Experimental Results

11 Methods

The first experiments were supposed to ensure the working of the amplifier. We connected an adjustable power supply and a $10\,\mathrm{G}\Omega$ resistance in series to the two inputs. The corresponding output voltages for the input voltage could be read out with a voltage meter or an oscilloscope. As mentioned above, we noticed that the amplifier performed insufficiently for our purpose. Nevertheless, we used it in our first attempts to measure the tunneling current.

The experimental setup for the experiments with the STM incorporated the following: the mechanical body of the STM, a battery to provide a stable bias voltage, the amplifier and two power supplies – one to power the amplifier and one to control the z-piezo. We used a Highly Ordered Pyrolytic Graphite (HOPG) sample and a piece of platinum-iridium wire as the tip, which we had both received from Dr. Thomas Jung (PSI, Uni Basel). Already in the first few attempts, we succeeded in detecting the tunneling current. However, the signal was too unstable to examine its properties.

After we had made the improvements mentioned in the documentation, we finally managed to get a rather stable signal. Computer connectible voltage probes and the software *Logger Pro* immensely simplified the measurements. The probes could be borrowed from our school, however, they had a range from only $-10\,\mathrm{V}$ to $+10\,\mathrm{V}$. This seemed sufficient for the amplifier output which has a maximum output voltage of about $14\,\mathrm{V}$. In contrast, the voltage at the z-piezo ranged from $0\,\mathrm{V}$ to $32\,\mathrm{V}$. A simple voltage divider built from a potentiometer solved the problem, dividing the voltage by four. This could be reversed on software basis in *Logger Pro*.

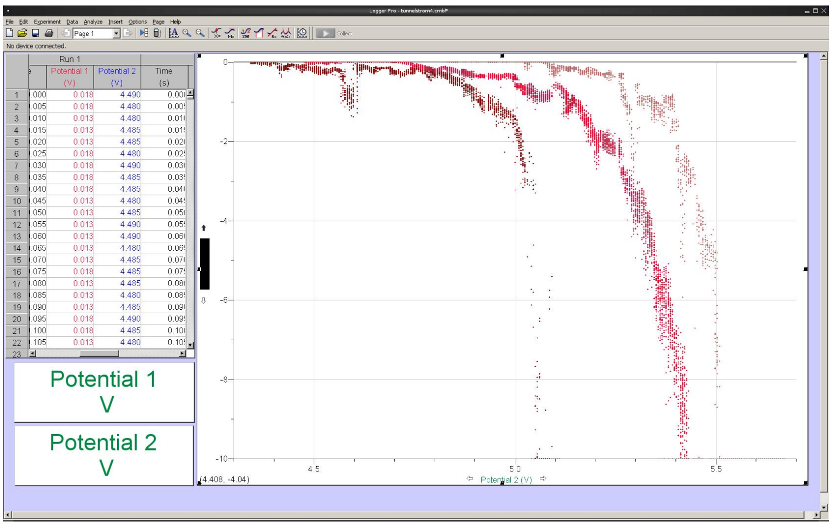

Figure 23: Computer-based measurement turned out to be very helpful – a screenshot of *Logger Pro*. Own picture.

12 Results

Figure 24 shows two graphs we obtained from a very good measurement. In the lower graph, the output voltage is logarithmized, very well illustrating the exponential relationship between tunneling current and distance.

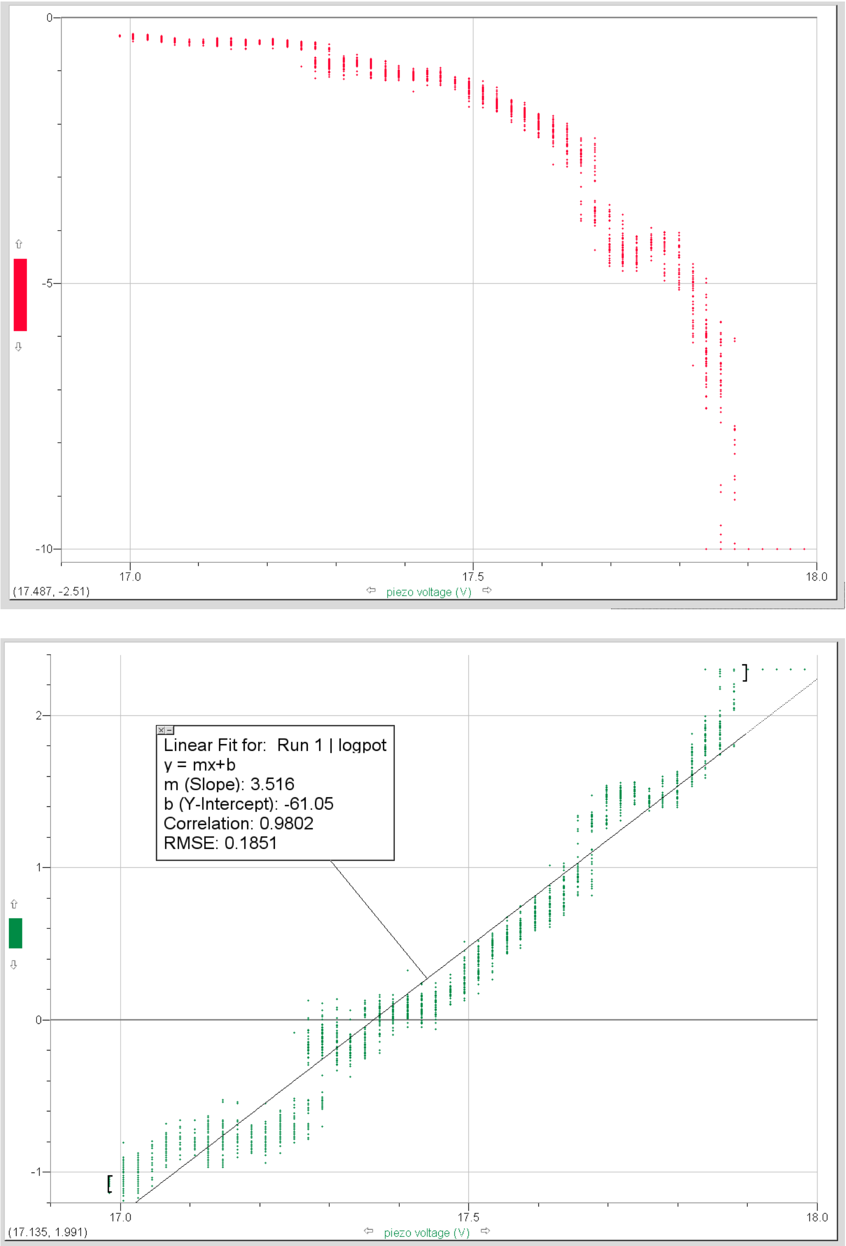

Figure 24: The two images show the results of one of our best measurements. The upper graph plots the output voltage over the voltage at the piezo (both in Volts) – in the lower one the output voltage is logarithmized. Own pictures.

Our amplifier as an input-output ratio of $10\,\frac{\mathrm{nA}}{\mathrm{V}}$. The gap between tip and sample linearly depends on the voltage at the piezo. The maximal stroke of the piezo according to the specifications is $5\,\mu$m at a voltage of 150 V so the expansion coefficient, call it ρ, is $\frac{100\,\mathrm{nm}}{3\,\mathrm{V}}$. Using these values, we can also draw a current-position graph and a logarithmized current-position graph. Note: The z-values are not the distance from the probe and can only be interpreted as relative distances.

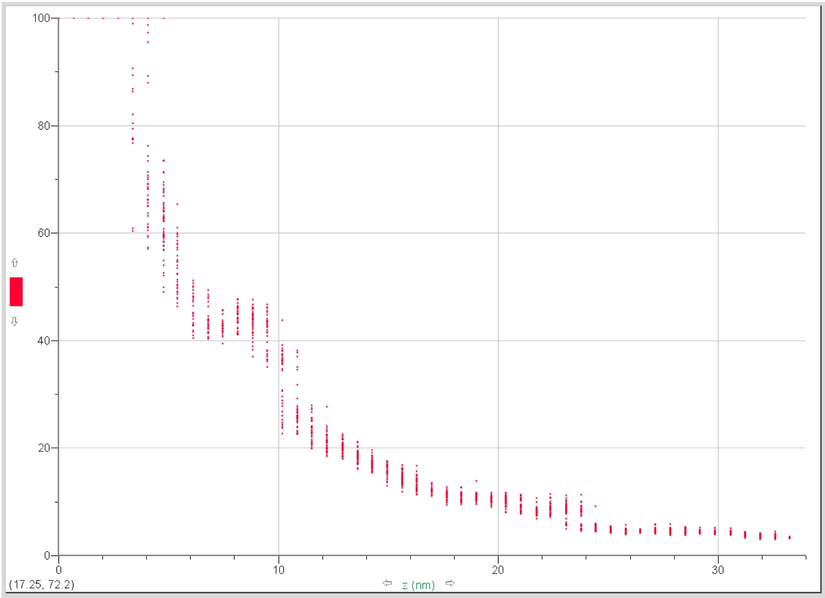

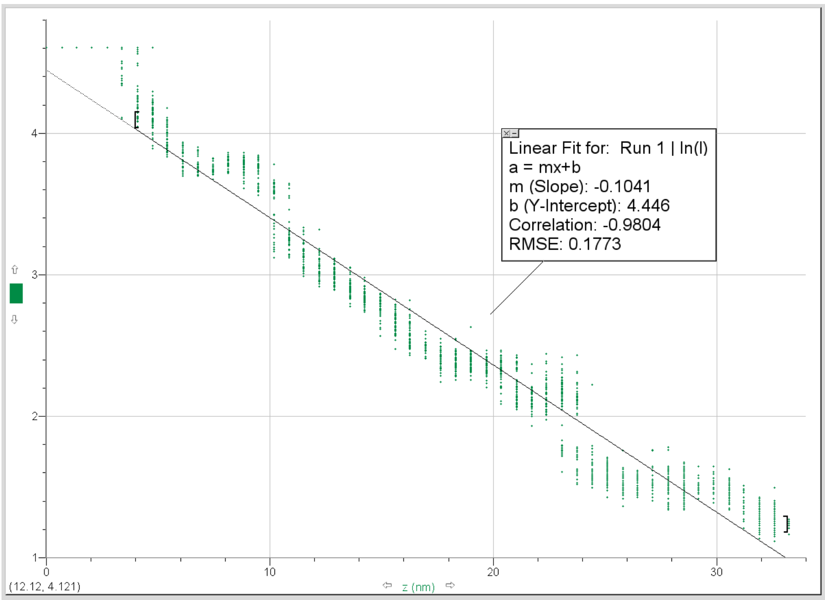

Figure 25: The same measurement as above but now with the values for current (in nA) and distance (in nm). Own pictures.

In section 2, we showed that the tunneling current I is proportional to $e^{-2\kappa d}$, with $\kappa = \frac{\sqrt{2m_e\phi}}{\hbar} = 1.087 \cdot 10^{10}\,\frac{1}{\mathrm{m}}$. One receives this numerical value with a workfunction equal to 4.5 eV, which is the approximate value for HOPG. We can use the slope in Figure 25 to check correlation between theory and experiment.

$$I_{out} = I_0\, e^{-2\kappa d}$$
$$\ln I = \ln I_0 - 2\kappa d$$
$$\frac{\mathrm{d}\, lnI}{\mathrm{d}\, d} = -2\kappa$$

This means the slope in the lower graph in Figure 25 should be equal to $-2\kappa = 2.17 \cdot 10^{10}\,\frac{1}{\mathrm{m}} = 21.7\frac{1}{\mathrm{nm}}$. This is much greater than the measured value, by about a factor 200. With the same values, a work function $\phi = 1 \cdot 10^{-4}\,\mathrm{eV}$ can be calculated. This is four orders of magnitude smaller than the actual value. The slope was between about $0.06\,\frac{1}{\mathrm{nm}}$ and $0.18\,\frac{1}{\mathrm{nm}}$ in our measurements.

As our results are reproducable, we had to find explanation for such a big discrepancy. After asking him for help, Dr. Thomas Jung from PSI gave us the hint that when operating in air, water will condensate on the sample. This severly influences the work function of the material. From [5]:

> Tunneling microscopy had long since entered the scientific arsenal as a precision instrument for the exploration of nanostructure of the surface of conducting materials. At the same time, the twenty-year experience of using scanning tunneling microscopes (STM) has unequivocally demonstrated that, when operating in air (ex situ) or in solutions (in situ), the behavior of the STM gap is impossible to describe by relationships intended for the electron tunneling in a vacuum. For example, the height of the tunneling barrier, when formally evaluated from the data of the tunneling-spectroscopy measurements in air with formulas for a vacuum tunneling gap is a few orders of magnitude as low as that obtained when performing measurements in a vacuum. At the same time, the resolution reached by an STM operating in air falls as a rule far short of that in a vacuum or even in solutions.
>
> Specifics of the ex situ operation of STM is defined by the formation of a thin layer of condensed moisture in the gap. The layer is in fact an electrolyte of an indefinite composition. The condensate on the surface was in some cases observed experimentally. When moved in, the STM tip is as a rule immersed into such a layer and the gap current has an electrochemical origin. As a result, at the same specified values of current, the tip-sample distance in the ex situ STM configuration happens to be far greater than in vacuum (or low-temperature) STM.

Drawing from the source, we can deduce that the big discrepancy between theory and experiment is due to the humid environment whereas the different values of the measured slopes can be attributed to an error in measurement. This is rather obvious, considering that even the graph of good measurements is rather a bar than a line and that external influences are still noticeable.

Sudden jumps of the current posed a frequent problem (Figure 26). Concluding from the quotation above, it seems probable that the tip moves into the condensate when the current jumps. Forces between the tip and the sample can also contribute to this problems. It is known that the attractive force between the tip and a HOPG sample can deform the sample [3].

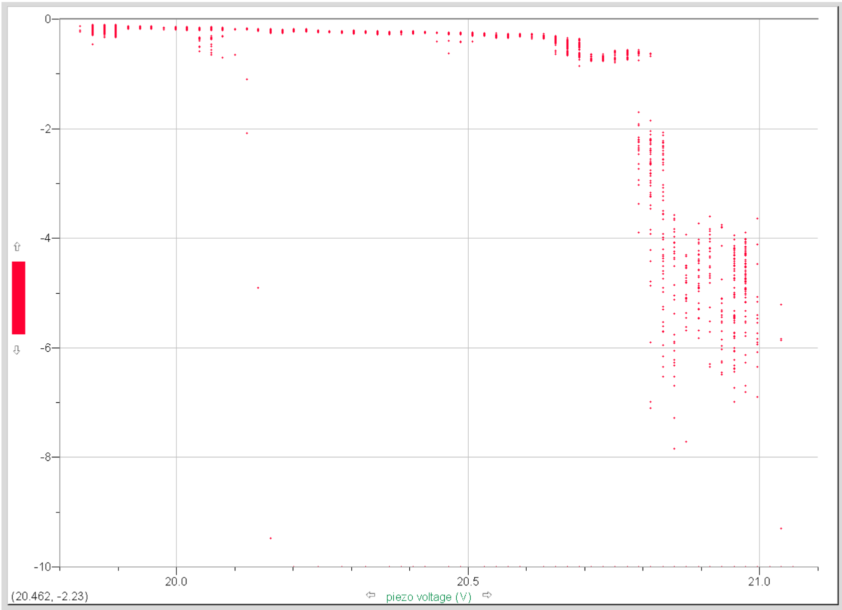

Figure 26: The tunneling current remains almost constant until it makes a sudden jump. Own picture.

Conclusion

In the course of the past six months, we have been investing major portions of our time for this, many would say, daring project of building such a device. It has involved a lot of hard work, patience and a lot of help from all sides. It has also taken a great deal of organisational work to pull this through. But we have had a great time, trying to master this challenge we have set before us. It has been fascinating to be able to create such an instrument and a great opportunity to immerse ourselves in this area of physics, closely related to nanotechnology, a topic which is on everyone's lips nowadays. We have discovered what it's like to be engaged in a scientific pursuit and how captivating such research can be. A further interesting aspect of our work was the development of solutions to the various problems, which inevitably arise in the course of such a large project.

Despite the fact that we did not succeed in accomplishing the fully functional microscope as we initially hoped to, we do not plan on giving up this project and it is our wish and ambition to continue working in the same direction and achieve the goal we have set before us.

References

[1] Chen, C. Julian. 1993.
Introduction to Scanning Tunneling Microscopy.
Oxford University Press. New York.

[2] Jia, Jin-Feng; Yang, Wei-Sheng and Xue, Qi-Kun.
Scanning Tunneling Microscopy.
In: Yao, Nan and Wang, Zhong Lin (Publ.). Handbook of Microscopy for Nanotechnology.
Kluwer Academic Publisher. New York.

[3] Kusunoki, Kouji; Sakata, Ichiro; Miyamura, Kazuo.
Interaction between Tip and HOPG Surface Studied by STS.
In: Analytical Sciences 2001, Vol.17 Supplement, i1267-i1268.

[4] Park, Sang-il and Barrett, Robert C. (1993).
Design Considerations for An STM System.
In: Stroscio, Joseph A. and Kaiser, William J. (Publ.). Scanning Tunneling Microscopy.
Academic Press, Inc. San Diego.

[5] Yusipovich, A. I.; Vassiliev S. Yu.
Voltage–Height Spectroscopy in the Ex Situ Configuration of a Scanning Tunneling Microscope.
In: Russian Journal of Electrochemistry, Vol. 41, No. 5, 2005, pp. 510–521.

[6] Jürgen Müller
An Amateur Scanning Tunneling Microscope.
http://www.e-basteln.de/ (January 8, 2009)

[7] *Piezoelectricity.*
http://en.wikipedia.org/wiki/Piezoelectricity (January 8, 2009)

[8] *Piezomechanik GmbH.*
http://www.piezomechanik.com (January 8, 2009)

[9] Dreyer, Hans Peter; Brovelli, D.; Cornaz, A.;
Dünki, R.; Lohe, H.-J.
Raster-Tunnel-Mikroskop (Leitprogramm).
http://www.educ.ethz.ch/lehrpersonen/physik/unterrichtsmaterialien_phy/modernephysik/raster_tunnel/index (January 8, 2009)

[10] *SXM Project.*
http://sxm4.uni-muenster.de/stm-de (January 8, 2009)

[11] *Work function.*
http://en.wikipedia.org/wiki/Work_function (January 8, 2009)